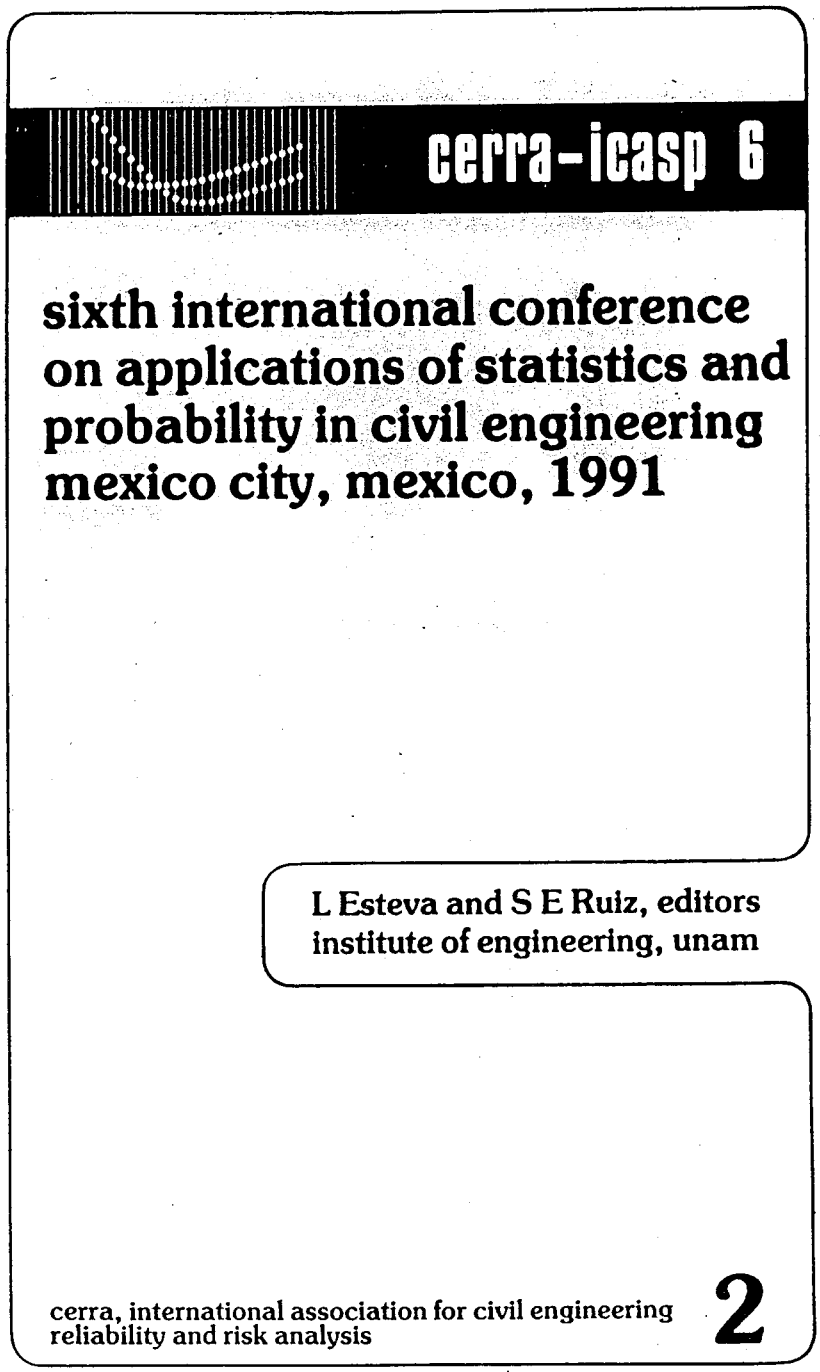

Volume 1 - ISBN 968-36-1976-2
Volume 2 - ISBN 968-36-1977-0
Set - ISBN 968-36-1975-4

Information address:
Institute of Engineering, UNAM
Ciudad Universitaria
Apartado Postal 70-472, Coyoacán
04510 México, D.F.
Mexico
Fax: (525) 548-3044

Ditlevsen, Ove and Gluver, Henrik:

Parameter estimation and statistical uncertainty in random field representation of soil strengths.

693-704.

PARAMETER ESTIMATION AND STATISTICAL UNCERTAINTY IN RANDOM FIELD REPRESENTATIONS OF SOIL STRENGTH

Ove Ditlevsen and Henrik Gluver
Dept. of Structural Eng., Techn. Univ. of Denmark, Build. 118, DK 2800 Lyngby, Denmark

Abstract Recent reliability evaluations of large foundations on saturated clay tills motivate an elaborated random field model for the variation of the "true" undrained shear strength over the relevant soil body upon consolidation. The generic set of candidate functions for the interpolation between the given cone tip resistance profiles (CPT profiles) is of operational reasons taken to be the set of sample functions of a homogeneous, horizontally isotropic and vertically Markovian logarithmic normal random field. Its probability densities are defined by four parameters (mean, variance, and two correlation parameters) modeled to be Bayesian random variables for which a posterior distribution is obtained by use of the given CPT profiles. Conditioning on the CPT profiles gives an inhomogeneous random field which is compared to measured vane shear strengths at given points of the soil body. Probabilistic models for the uncertainties of each of the two independent measuring methods tied together by an assumption of proportionality between the "true" cone tip resistance and the "true" vane shear strength lead to the operationally simplest possible statistical model for making the comparison. This model introduces three more Bayesian random variables, the proportionality factor, the variance reduction factor, and the variance of the vane test measuring error, of which the two first are applied on the inhomogeneous CPT field in order to transform it into the "true" in situ shear strength field. Finally a non–standard interpretation of the triaxial compression test gives the information needed to define a random transformation of the "true" in situ shear strength field into the "true" shear strength field as it is assumed to exist upon the termination of the consolidation from the weight of the structure. It is concluded that a manageable random field model is available for the undrained shear strength embracing the relevant soil strength data in terms of some few Bayesian random variables that can be included in practicable automatic foundation reliability computations.

Introduction In an actual case of a reliability analysis of the large foundations on saturated clay till of the anchor blocks for the future suspension bridge across the eastern channel of Storebælt in Denmark (main span = 1624m) a considered failure mode is an undrained failure in the clay till. Fig. 1 shows one of the tender designs to the western anchor block. An undrained failure is modeled by ideal plasticity theory with the undrained shear strength of the clay till defining the yield limit. The considered rupture figure is cylindrical and composed by surface failures, Prandtl zones (radial zones) and Rankine zones (triangular zones) as indicated in Fig. 1. The length of the cylinder equals the width of the footing. For a unit angular velocity the plastic dissipation has the form

$$D = r \int_{\mathscr{S}} c_u + \int_{\mathscr{R}} c_u + \int_{\mathscr{P}} \frac{r+s}{dist} c_u \qquad (1)$$

except for the end contributions. The generic symbols r and s are defined in Fig. 1 while c_u is the undrained shear strength field, $\mathscr{S}$ is the total outer surface between the moving soil and the resting soil not including the ends, $\mathscr{R}$ is the soil body occupied by Rankine zones, and $\mathscr{P}$ is the soil body occupied by Prandtl zones. The symbol "dist" is the distance within the actually considered Prandtl zone (radial zone) between the pole axis and the point at which c_u is considered.

The dissipation obtained from (1) plus the end contributions is an upper bound on the dissipation obtained from the weakest rupture figure among the set of all kinematically

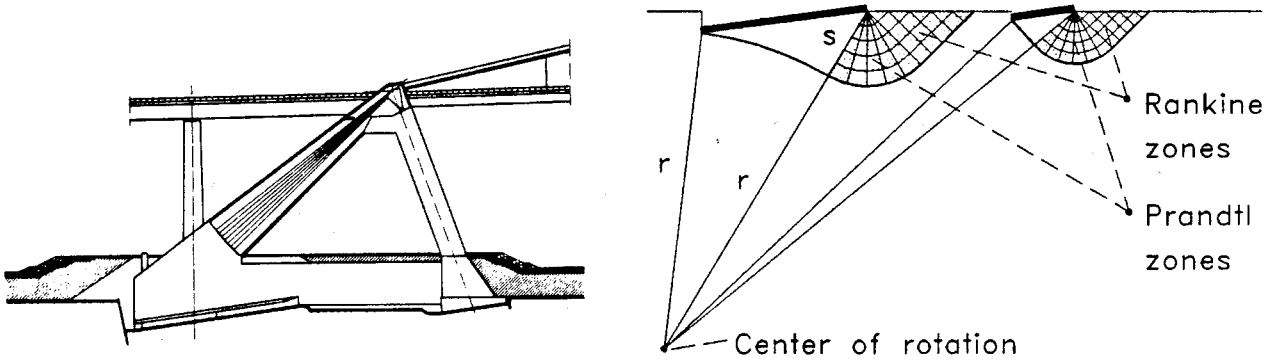

Fig. 1. Tender design for in situ built anchor block for the suspension bridge across the eastern channel of Storebælt. The block is a rigid structure supported by two rigid rectangular foundations of dimensions 22×50 m (front) and 55×51 m (rear). The distance from rear end to front end is 125 m and the height is 71 m. A possible rupture figure with respect to undrained failure is shown to the right.

possible spatial rupture figures given that the external work rate is kept the same. For a semi–circular footing a class of kinematically possible rupture figures are the spherical rupture surfaces that cut the foundation level at the circular part of the boundary of the footing. Assuming that the carrying capacity of a uniformly vertically loaded semi–circular footing and of a rectangular footing of the same area and with the side ratio 1 to 2 is about the same, Brinch Hansen (1966) found that the minimal dissipation obtained from (1) only requires a minor correction of the dissipation in order to give the same minimal dissipation as in the class of spherical surface ruptures. On this basis Brinch Hansen suggested that the dissipation could be put to $[1+J\ \text{area}(\mathscr{C})/\text{area}(\mathscr{S})]D$, where $\mathscr{C}$ is the cross section of the rupture cylinder and J is a judgmental factor about 0.5. The formula is correct for $\text{area}(\mathscr{S}) \to \infty$ corresponding to a strip foundation. Data from model tests with vertical loading on rectangular footings support the correction factor (shape factor) 1 + 0.2 (width/length), where "width" = smallest side of the footing, "length" = largest side of the footing, Skempton (1951). For $J \simeq 0.5$, the correction factor becomes reasonably consistent with Skempton's empirical result. For inclined loading the correction factor decreases with the horizontal load component and it becomes 1 for pure horizontal loading, in which limit the rupture corresponds to a sliding failure. In the reliability analysis J may be modeled as a normally distributed random variable of mean 0.5 and a coefficient of variation which by professional geotechnical judgment is assessed to be about 5 to 10%.

Each of the integrals in (1) are sums of integrals of c_u over simple rectangles (for $\mathscr{S}$) or simple triangular prisms (for $\mathscr{R}$ and $\mathscr{P}$) when the integrations are performed in suitably chosen coordinate systems. For example, each Prandtl zone has a polar axis. Taking this as polar axis of a semi–polar coordinate system, the denominator "dist" cancels out by the proportionality with "dist" of the volume element. Thus the integral is reduced to an integral of c_u over a prism in the space of the semi–polar coordinates. These simple shapes of

the integration domains make it simple to apply Monte Carlo integration technique.

In the actual reliability analysis the c_u field is modeled as a random field with a mean value function $E[c_u(\mathbf{x})]$ and a covariance function $Cov[c_u(\mathbf{x}_1),c_u(\mathbf{x}_2)]$. Thus with obvious symbolism

$$E[D] = \left[r\int_{\mathscr{S}} + \int_{\mathscr{R}} + \int_{\mathscr{P}} \frac{r+s}{dist(\mathbf{x})}\right] E[c_u(\mathbf{x})] \tag{2}$$

$$Var[D] = \left[r_1\int_{\mathscr{S}_1} + \int_{\mathscr{R}_1} + \int_{\mathscr{P}_1} \frac{r_1+s_1}{dist(\mathbf{x}_1)}\right]\left[r_2\int_{\mathscr{S}_2} + \int_{\mathscr{R}_2} + \int_{\mathscr{P}_2} \frac{r_2+s_2}{dist(\mathbf{x}_2)}\right] Cov[c_u(\mathbf{x}_1),c_u(\mathbf{x}_2)] \tag{3}$$

where $\mathscr{S}_1$ indicates integration with respect to $\mathbf{x}_1 \in \mathscr{S}$ and $\mathscr{S}_2$ indicates integration with respect to $\mathbf{x}_2 \in \mathscr{S}$ and similarly for $\mathscr{R}$ and $\mathscr{P}$. For the rupture figure in Fig. 1 there are 10 double and triple integrals in (2) over rectangles or triangular prisms while there correspondingly are 55 4–double, 5–double or 6–double integrals in (3) over cartesian products of rectangle with rectangle, rectangle with triangular prism, or triangular prism with triangular prism. In principle all of these integrals can be computed easily by Monte Carlo technique up to a specified accuracy of the evaluation of E[D] and Var[D] in terms of sampling standard deviations. It is clear that this computation may become prohibitly computer time consuming if the accuracy requirements are specified too narrow. However, consistently with the philosophy of structural reliability analysis, uncertainty due to the use of a limited sample of random points in the Monte Carlo simulation can be included in the analysis in the same way as the statistical uncertainty originating from only having available a limited sample of measurements of a relevant physical property. In any case, the size of the generated sample must be large enough to reach stability of the estimates of E[D] and Var[D] and also be large enough to allow the assumption of normal distribution modeling of the uncertainty.

In the following a stochastic field model is formulated for c_u. It will embrace all the relevant information obtained by measuring cone tip resistances (CPT measurements) and vane shear strengths in situ and by making triaxial undrained compression experiments on samples of clay till in the laboratory. Several parameters Θ_1,... (means, standard deviations, correlation lengths, etc.) are needed to define the field. For given values of these parameters the field is assumed to be of sufficient random variability across the rupture surfaces and zones to justify the assumption that D conditional on Θ_1, ... has a normal distribution irrespective of the distribution type for c_u at any point. The mean and the variance of D given fixed values of the parameters are obtained from (2) and (3). The probability of undrained failure in the considered failure mode is then the probability of the event

$$\left[1+I\frac{area(\mathscr{C})}{area(\mathscr{S})}\right]\left\{E[D|\Theta_1,...] + U\sqrt{Var[D|\Theta_1,...]}\right\} - W < 0 \tag{4}$$

in which U is a standard normal random variable and W is the external work rate which may be a random variable due to randomness of or incomplete knowledge about the external

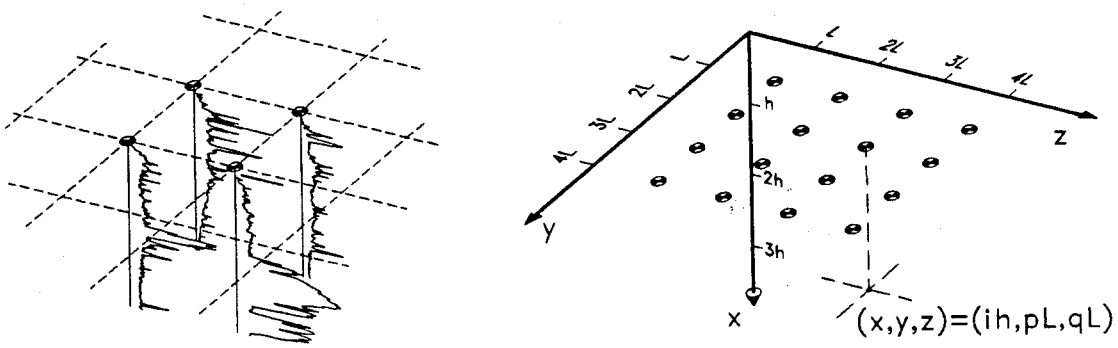

Fig. 2. Examples of measured vertical cone tip resistance profiles (CPT) and definition of the coordinate system and measuring mesh to which the filtered and smoothened cone tip resistances are referred.

loads. The parameters Θ_1, ... are Bayesian random variables that model the uncertainty in the interpretation of the soil strength measurements in terms of the field of undrained shear strengths.

The rest of the paper deals with this random field modeling which will be explained in terms of the actual example from Storebælt. The random field of undrained shear strengths c_u upon consolidation is modeled in 4 steps. First step is a formulation of a homogeneous random field of cone tip resistances q_c on the basis of a statistical analysis of 60 CPT filtered and smoothened cone tip resistance profiles obtained in a rectangular mesh of 6 times 10 points in the horizontal plane with a distance of 20 m between the points in both directions of the mesh, Fig. 2. Second step is the determination of the inhomogeneous random field of q_c from the homogeneous field by conditioning on the measured q_c profiles (kriging). Third step is the formulation of a model for transformation of the inhomogeneous q_c field into a field of "true" in situ undrained shear strength c_u. This formulation is based on a particular statistical technique of determining the measuring uncertainties of two different measuring methods that are applied to the same object. Here this object is the true in situ undrained shear strength and the two measuring methods are the CPT and the vane test. Fourth step is a transformation of the true in situ undrained shear strength field into the random field of increased shear strengths caused by the consolidation of the clay till by the permanent stress increments from the structure. The formulation of this transformation is based on a statistical analysis of data from triaxial tests.

First step: Homogeneous random field model of CPT cone tip resistances Let $\xi(x,y,z)$ denote log q_c at (x,y,z) where x,y, and z refer to the coordinate system shown in Fig. 2. Assume that ξ is a homogeneous and horizontally isotropic Gaussian field with

$$E[\xi(x,y,z)] = \mu,\ Cov[\xi(x_1,y_1,z_1),\xi(x_2,y_2,z_2)] = \sigma_0^2 e^{-\alpha|x_1-x_2|} e^{-\beta[(y_1-y_2)^2+(z_1-z_2)^2]} \quad (5)(6)$$

in which μ, σ_0, α, β are unknown parameters. These parameters are to be evaluated by the Bayesian statistical method on the basis of the given CPT–data. The reason for the specific

choice (6) of covariance function will be explained subsequently.

In order to reduce the amount of data in the computations down to a manageable size the field is averaged over disjoint intervals in the vertical direction. The average is taken over the length h of the vertical mesh interval and the averaged value is denoted by ζ_{ipq} where the triple (i,p,q) of integers label the mesh point in the spatial mesh indicated in Fig. 2. Since the averaging are over disjoint intervals, the Markov process property of ξ in the vertical direction as introduced by (6) is preserved approximately in the sequence ζ_{1pq}, ζ_{2pq}, ... for each (p,q) provided $\alpha h << 1$. We have the exact covariance

$$\mathrm{Cov}[\zeta_{ipq},\zeta_{jrs}] = \sigma_h^2 \, \rho^{|i-j|} \, \kappa^{(p-r)^2+(q-s)^2} \quad \text{for } i \neq j \tag{7}$$

where $\sigma_h^2 = \sigma_0^2 \, 2[\cosh(\alpha h)-1]/(\alpha h)^2 \simeq \sigma_0^2$ for $\alpha h << 1$, $\rho = \exp[-\alpha h]$, $\kappa = \exp[-\beta L^2]$, with h = 0.1 m, say, and L = 20 m. In the following we denote σ_h by σ. With given measurements of ζ_{ipq} (i = 1, ..., m; p = 1, ..., l; q = 1, ..., k) (m = 150, l = 10, k = 6 for Storebælt Anchor Block West) and according to the Bayesian statistical method the values of the parameters μ, σ, ρ, κ are assessed by studying the likelihood function. Computation of the joint Gaussian density of the m × l × k (= 9000) random variables ζ_{ipq} requires the inversion of the corresponding huge covariance matrix containing the unknown parameters. Generally this is prohibitive for applying likelihood function studies of random field parameter uncertainties. Recourse must generally be taken to "boot strapping" simulation studies. However, for the particular covariance function in (6) it is possible to factorize the covariance matrix in a special way that allows the inversion of it by numerical inversion of two matrices of order l and k respectively and both having the same mathematical form. Without giving details here, Ditlevsen (1991a), we state that the random variables ζ_{ipq} can be ordered in a column matrix ζ such that the covariance matrix of ζ can be written $\mathrm{Cov}[\zeta,\zeta'] = \sigma^2[[S_2]\circ S_1] \circ P$ in which

$$\mathbf{P} = \begin{bmatrix} 1 & \rho & \rho^2 & \dots & \rho^m \\ \rho & 1 & \rho & \dots & \rho^{m-1} \\ \dots & & & & \end{bmatrix}, \quad \mathbf{P}^{-1} = \frac{1}{1-\rho^2}\begin{bmatrix} 1 & -\rho & 0 & \dots & 0 \\ -\rho & 1+\rho^2 & -\rho & \dots & 0 \\ \dots & & & & \end{bmatrix}, \quad \mathbf{S}_i = \begin{bmatrix} 1 & \kappa & \kappa^4 & \dots & \kappa^{(\nu-1)^2} \\ \kappa & 1 & \kappa & \dots & \kappa^{(\nu-2)^2} \\ \dots & & & & \end{bmatrix} \tag{8)(9)(10}$$

where **P** is the correlation matrix for the vertical Markov sequence, and $\mathbf{S}_i$ for i = 1 (ν = l) and i = 2 (ν = k) are the correlation matrices in the two horizontal directions of the mesh respectively. The "bracket and ∘" symbolism stands for a special matrix product where the matrix outside the bracket is applied as a multiplicator on each single element of the matrix inside the bracket forming a matrix of order equal to the product of the orders of the two matrices. Thus, with $\mathbf{A} = \{a_{ij}\}$ we have $[\mathbf{A}] \circ \mathbf{B} = \{a_{ij}\,\mathbf{B}\}$. It can be shown generally that if **A** and **B** are correlation matrices (non–negative definite matrices) then $[\mathbf{A}] \circ \mathbf{B}$ is a correlation matrix. Also, if **A** and **B** are regular matrices, then $[\mathbf{A}] \circ \mathbf{B}$ has the inverse matrix $[\mathbf{A}^{-1}] \circ \mathbf{B}^{-1}$. Moreover, $\det([\mathbf{A}] \circ \mathbf{B}) = (\det \mathbf{A})^{\text{order B}} (\det \mathbf{B})^{\text{order A}}$. Using these properties it is

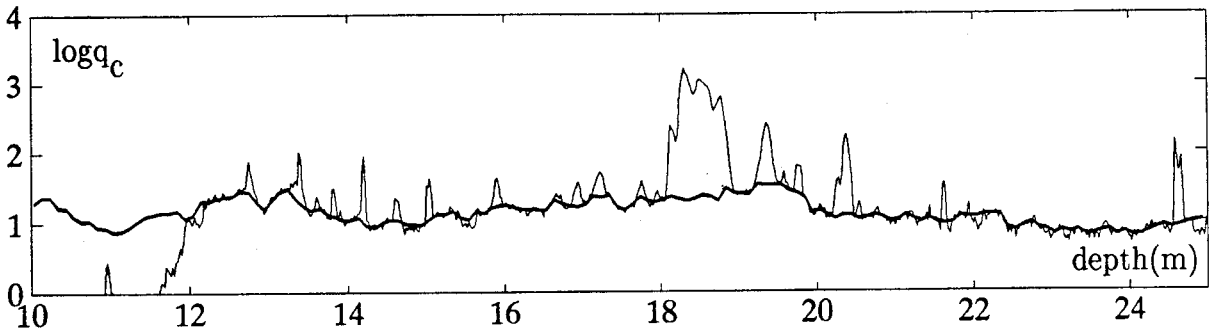

Fig. 3. Raw logarithmic cone tip resistance profile (thin curve) and the "cleaned" (filtered) and smoothed $\log q_c$*–profile (thick curve).*

possible to formulate and study the likelihood function

$$L(\mu,\sigma,\rho,\kappa|\,\zeta) \propto (\det \mathbf{C})^{-1/2} \exp\left[-\tfrac{1}{2}(\zeta-\mu\,\mathbf{e})'\,\mathbf{C}^{-1}(\zeta-\mu\,\mathbf{e})\right] \tag{11}$$

in which $\mathbf{e}' = [1 \ldots 1]$ and $\mathbf{C} = \mathrm{Cov}[\zeta,\zeta']$.

The Bayesian random variables corresponding to the parameters μ, σ, ρ, κ are denoted by M, Σ, P, K respectively and it is assumed that the prior density of (M,log Σ,P,K) is diffuse over $\mathbb{R}^2 \times [0,1]^2$. Thus the posterior density of the parameters are obtained by multiplying the likelihood function by $1/\sigma$. Defining

$$N(P,K)=\mathbf{e}'\mathbf{C}^{-1}\mathbf{e},\ \mathrm{wav}(P,K)=\frac{\mathbf{e}'\mathbf{C}^{-1}\zeta}{N(P,K)},\ s(P,K)^2=\frac{N(P,K)}{\mathbf{e}'\mathbf{e}}\left[\frac{\zeta'\mathbf{C}^{-1}\zeta}{N(P,K)}-\mathrm{wav}(P,K)^2\right] \tag{12)(13)(14}$$

("wav" = weighted average) it follows from the joint posterior density obtained from (11) that the random variables

$$[M-\mathrm{wav}(P,K)]\sqrt{N(P,K)}\,/\,\Sigma \ \text{ and } \ \mathbf{e}'\mathbf{e}\,s(P,K)^2\,/\,\Sigma^2 \tag{15)(16}$$

and the random pair (P,K) are mutually independent with the first being standard normal and the second being χ^2–distributed with $\mathbf{e}'\mathbf{e} - 1 = \mathrm{mlk} - 1$ degrees of freedom. For the Storebælt data we have mlk = 9000, which is so large that the coefficient of variation of the corresponding χ^2–variable is only about 1.5%. Therefore it is sufficiently accurate for the purpose to replace χ^2 with the constant $\mathbf{e}'\,\mathbf{e}$ $(= 1 + \mathrm{E}[\chi^2])$. Thus we have

$$M \simeq U_1\,\Sigma/\sqrt{N(P,K)} + \mathrm{wav}(P,K) \ \text{ and } \ \Sigma \simeq s(P,K) \tag{17)(18}$$

in which U_1 is a standard normal random variable.

The data in ζ are obtained from the CPT–measurements as follows. First the raw cone tip resistance data are "cleaned" for outlaying observations interpreted as effects of stones or voids (weak spots) distributed at random in the till body. This cleaning is made by an auto-

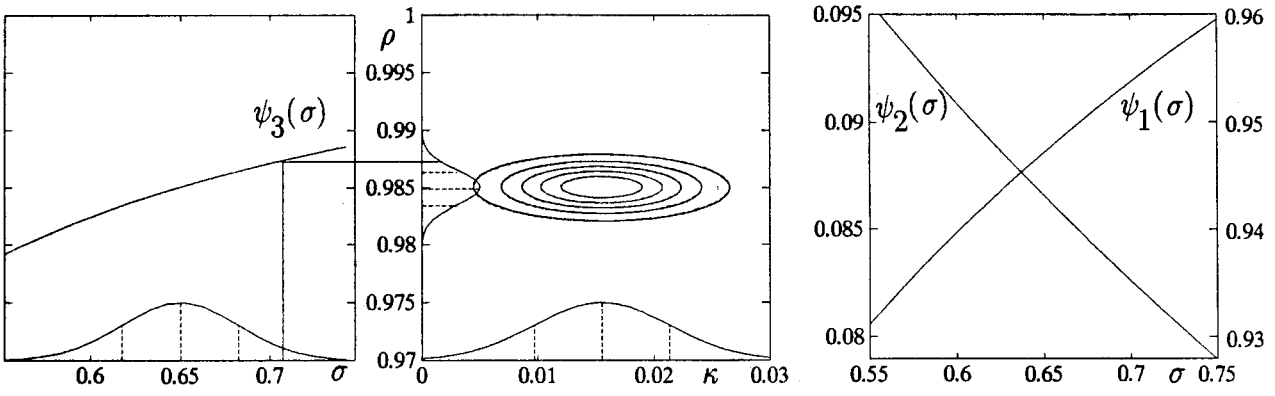

Fig. 4. Contour curves (middle diagram) in full line for the joint density of the correlation parameters (K,P) *together with the marginal densities of* K *and* P *shown along the abscissa axis and the ordinate axis respectively. The dotted contour curves are for the density function obtained as the product of the two marginal density functions. The diagram to the left shows the density of the standard deviation* Σ *and the transformation function* $\rho = \psi_3(\sigma)$ *between* Σ *and* P. *The diagram to the right shows the graphs of the two functions* $\psi_1(\sigma)$ *and* $\psi_2(\sigma)$ *in (19). All marginal densities are well approximated as truncated Gaussian. The point estimates* $\rho = 0.984$, $\kappa = 0.016$ *correspond to correlation lengths of about* 6.2 m *in the vertical direction and* 8.7 m *in the horizontal direction.*

matic procedure based on likelihood arguments consistent with the Gaussian Markov process assumption introduced by the correlation structure (6) in the vertical direction. Dismissed observations are replaced by artificially generated observations obtained by Markov interpolation between the accepted observations. The procedure is explained in details in Ditlevsen (1991b). Finally the large amount of cleaned data is reduced by averaging over disjoint intervals of suitable length h (e.g. h = 10 cm, for Storebælt the raw observations are per 2 cm). An example of a cleaned and averaged CPT cone tip resistance profile is shown in Fig. 3. With these data substituted into ζ a numerical study of the marginal posterior density of (P,K) reveals that P and K with sufficient accuracy can be modeled to be mutually independent and both be truncated Gaussian, Fig. 4. In the domain of likely values of (ρ,κ) it turns out that $N(\rho,\kappa)$, $wav(\rho,\kappa)$, and $s(\rho,\kappa)$ are practically independent of κ. In particular the relation between Σ and P can be modeled as a one to one relation, Fig. 4 (left). Since ρ is bounded by 1, numerical convergence difficulties may show up in the automatic gradient based reliability computation if Σ is programmed to be a function of P. The problem is eliminated by letting P be a function of Σ.

The final result of the numerical study of the joint posterior distribution of the parameters is that the statistical uncertainty of the parameters are determined by the three mutually independent Bayesian random variables $\theta_1 = U_1$, $\theta_2 = \Sigma$, $\theta_3 = K$ where U_1 is standard Gaussian while Σ and K are truncated Gaussian, Fig. 5. The Bayesian random variables M, P are given by

$$M = U_1\, \psi_1(\Sigma)\, \Sigma + \psi_2(\Sigma) \quad \text{and} \quad P = \psi_3(\Sigma) \qquad (19)(20)$$

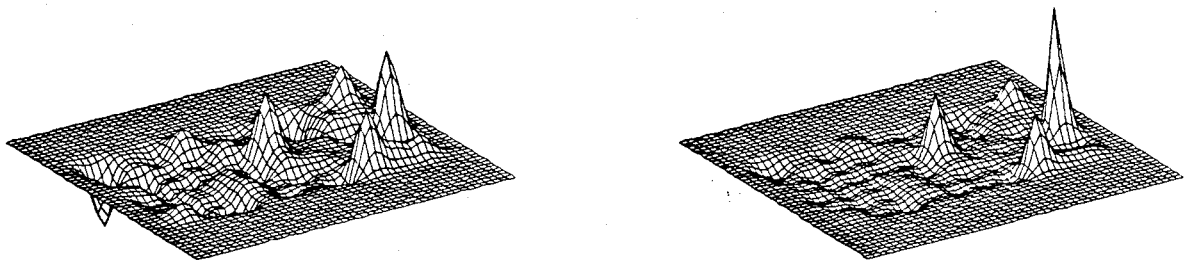

Fig. 5. Illustration of the variation of $E[\log q_c | \zeta,\mu,\sigma,\rho,\kappa]$ *(left) and* $E[q_c | \zeta,\mu,\sigma,\rho,\kappa]$ *(right)* $(q_c=\exp[\zeta(x,y,z)])$ *with respect to* y *and* z *at a fixed level* x.

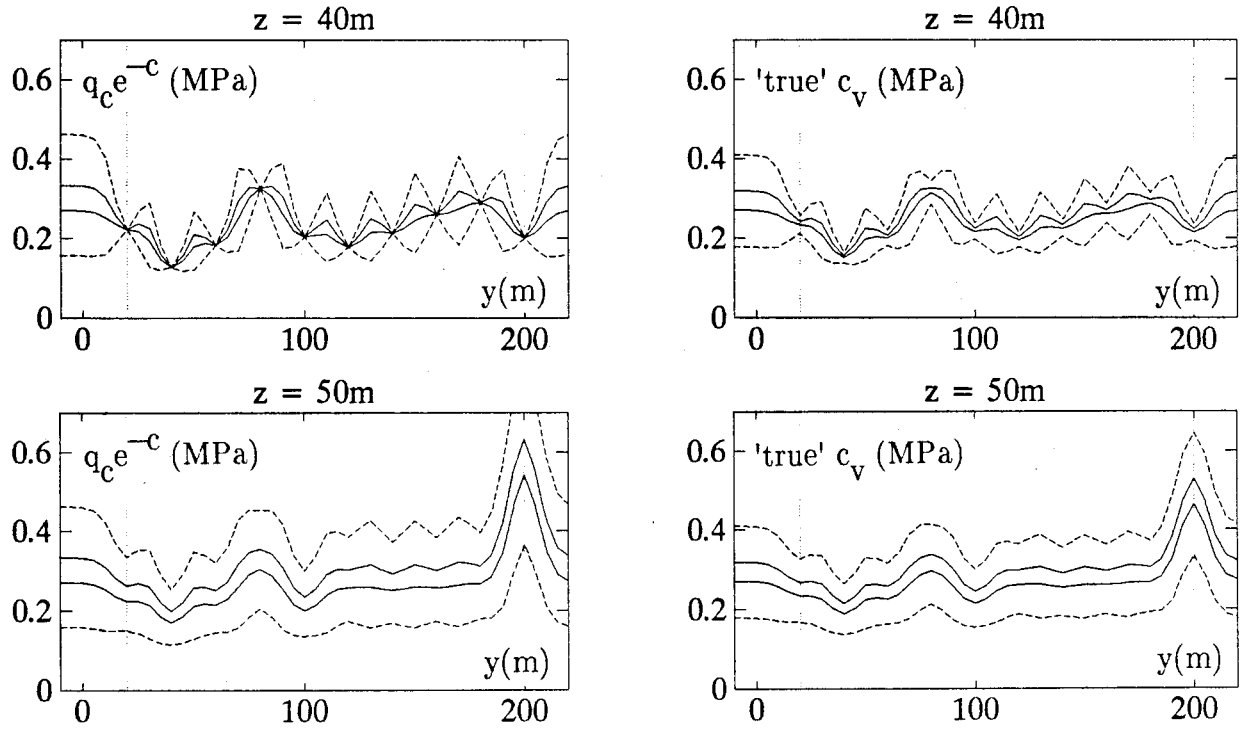

Fig. 6. Variation of conditional mean (upper full curve), median (lower full curve), 10% fractile (lower dotted curve), and 90% fractile (upper dotted curve) along a horizontal line through a row of mesh points (upper diagrams) and halfway between this and the next row of mesh points in the same horizontal plane (lower diagrams). The right diagrams are for the "true" undrained shear strength field while the left diagrams are for the q_c *field shown on a commensurable scale obtained by use of the factor* $\exp[-E[C]]$.

where ψ_1, ψ_2 are functions with graphs as shown in Fig. 4 (right) while ψ_3 has the graph shown in Fig 4 (left).

Second step: Kriging The conditional vertically averaged field $[\zeta(x,y,z) | \zeta,\mu,\sigma,\rho,\kappa]$ is inhomogeneous with the linear regression of $\zeta(x,y,z)$ on ζ as mean value function and the corresponding residual covariance function as covariance function. This conditional field represents together with the Bayesian distribution of the parameters the measured cone tip resistance information extended to the entire soil body. Due to the Markov property in the vertical direction, the linear regression only depends on those values in ζ that correspond to

the same level as x when we restrict x to the mesh points. The mean value function is with x = j h:

$$E[\zeta(jh,y,z)\,|\,\zeta,\mu,\sigma,\rho,\kappa] = \mu + \sum_{p=1}^{l}\sum_{r=1}^{l}\sum_{q=1}^{k}\sum_{s=1}^{k} \omega_{pr}(\kappa)\,\psi_{qs}(\kappa)\,\kappa^{(p-y/L)^2+(q-z/L)^2}(\zeta_{jrs}-\mu) \tag{21}$$

where ω_{pr} and ψ_{qs} are the generic elements in $\mathbf{S}_1^{-1}$ and $\mathbf{S}_2^{-1}$ respectively while ζ_{jrs} is the relevant element of ζ. In particular, the mean is ζ_{jrs} for y = rL and z = sL. The conditional covariance function is

$$\mathrm{Cov}[\zeta(ih,y_1,z_1),\zeta(jh,y_2,z_2)\,|\,\zeta,\mu,\sigma,\rho,\kappa] = \sigma^2\,\rho^{|i-j|}\Big\{\kappa^{[(y_1-y_2)^2+(z_1-z_2)^2]/L^2} - \sum_{p=1}^{l}\sum_{r=1}^{l}\omega_{pr}(\kappa)\kappa^{(p-y_1/L)^2+(r-y_2/L)^2}\sum_{q=1}^{k}\sum_{s=1}^{k}\psi_{qs}(\kappa)\kappa^{(q-z_1/L)^2+(s-z_2/L)^2}\Big\} \tag{22}$$

Fig. 5 shows the conditional mean of $\zeta(x,y,z)$ (left) and $\exp[\zeta(x,y,z)]$ (right) along a horizontal plane for the Storebælt data while Fig. 6 (left) shows the conditional mean, the median, the 10% fractile, and the 90% fractile for the one–dimensional conditional distributions along some selected lines parallel to the mesh, all for $\exp[\zeta(x,y,z)]$.

Third step: Transformation to in situ undrained shear strength field At any point of the soil body at which the in situ undrained vane shear strength c_v has been measured, $\log c_v$ can be compared to the distribution of $\log q_c$ as defined above by the conditional field $[\zeta(x,y,z)\,|\,\zeta,\mu,\sigma,\rho,\kappa]$. Elasto–plastic continuum mechanics predicts that there is almost proportionality between c_v and q_c for an ideal homogeneous saturated clay. Taking this as a "law", the observed large deviations of the pairs (c_v,q_c) from being situated on the same straight line through the origin must be attributed to measuring uncertainty. Acceptance of the proportionality law makes it possible to estimate the proportionality constant as well as the measuring uncertainty of both c_v and q_c in terms of probability distributions. This leads to the transformation of the random field of "measured" q_c values into the random field of "true" undrained shear strength values. The procedure is described in details in Ditlevsen (1991c). The main features are as follows:

Let $\mathbf{Z} = \mathbf{X} + \mathbf{Y} = \mathbf{X}_v + \mathbf{Y}_v + c\,\mathbf{e}$ be the vector of "true" values of $\log q_c$, $\mathbf{X}$ be the vector of "measured" values of $\log q_c$, $\mathbf{X}_v$ be the vector of measured values of $\log c_v$, and c be the additive transformation constant between the "true" values of $\log c_v$ and $\log q_c$. The vectors $\mathbf{Y}$ and $\mathbf{Y}_v$ contain the measuring errors of the two methods. The following modeling assumptions are made: $\mathrm{Cov}[\mathbf{Y},\mathbf{Y}_v'\,|\,\mathbf{Z}] = \mathbf{0}$, $E[\mathbf{Y}\,|\,\mathbf{Z}]$ and $E[\mathbf{Y}_v\,|\,\mathbf{Z}]$ are both independent of $\mathbf{Z}$,$\mathrm{Cov}[\mathbf{Y},\mathbf{Y}'] = \lambda^2\,\mathrm{Cov}[\mathbf{X},\mathbf{X}']$ with $0 \le \lambda \le 1$ (this assumption is equivalent to the assumption that the linear regression of the ith element of $\mathbf{Z}$ on $\mathbf{X}$ depends solely on the ith element X_i of $\mathbf{X}$ and

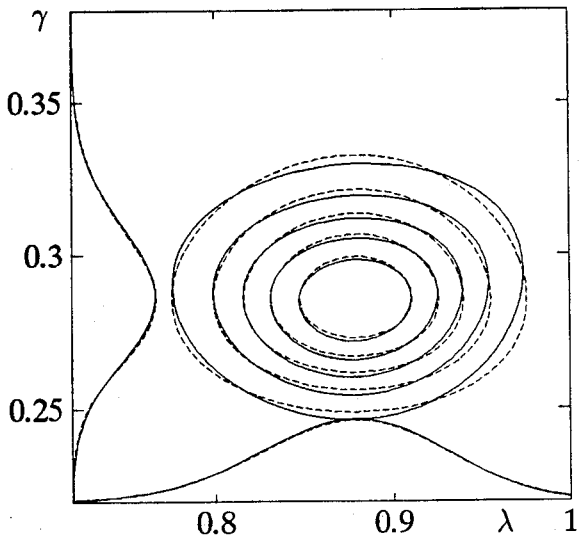

Fig. 7. Contour curves for the joint density of (Λ,Γ) *given that* $C = 2.255$ *(full line). The marginal densities of* Λ *and* Γ *are shown along the abscissa axis and the ordinate axis respectively (full lines). The approximating marginal density shown with dotted line is for* Λ *obtained from setting*

$$\Lambda^2 = (0.1134 + 0.00119\ V)^{-1} - 8.05$$

where V *is a lower truncated standard normal random variable truncated at* -2.439, *and for* Γ *it is a truncated Gaussian density. The dotted contour curves correspond to the product of the two marginal densities.*

that the regression coefficient is independent of i), $\mathrm{Cov}[\mathbf{Y}_v,\mathbf{Y}_v'] = \gamma^2\,\mathbf{I}$ ($\mathbf{I}$ = unit matrix, that is, the measuring errors in different vane tests are independent), $(\mathbf{Z},\mathbf{Y},\mathbf{Y}_v)$ is jointly Gaussian. A consequence of these assumptions is that the Gaussian density of $\mathbf{X}_v$ is

$$f_{\mathbf{X}_v}(\mathbf{x}_v) \propto \sqrt{\det\ \mathbf{R}(\gamma,\lambda)}\ \exp\left[-\tfrac{1}{2}\,\xi(c,\lambda)'\,\mathbf{R}(\gamma,\lambda)\,\xi(c,\lambda)\right],\ c \in \mathbb{R},\ \gamma \in \mathbb{R}_+,\ \lambda \in [0,1] \tag{23}$$

$$\xi(c,\lambda) = \mathbf{x}_v - \lambda^2 E[\mathbf{X}\,|\,\zeta] - [(1-\lambda^2)\mu - c]\mathbf{e} \tag{24}$$

$$\mathbf{R}(\gamma,\lambda) = [\lambda^2(1-\lambda^2)\mathbf{C}_{\mathbf{X}} + \lambda^4\mathbf{C}_{\mathbf{X}|\zeta} + \gamma^2\mathbf{I}]^{-1} \tag{25}$$

where $\mathbf{C}_{\mathbf{X}} = \mathrm{Cov}[\mathbf{X},\mathbf{X}']$ corresponds to the homogeneous field $[\zeta(x,y,z)\,|\,\mu,\sigma,\rho,\kappa]$ while $E[\mathbf{X}\,|\,\zeta]$, $\mathbf{C}_{\mathbf{X}|\zeta} = \mathrm{Cov}[\mathbf{X},\mathbf{X}'\,|\,\zeta]$ corresponds to the inhomogeneous conditional field $[\zeta(x,y,z)\,|\,\zeta,\mu,\sigma,\rho,\kappa]$.

In practice the set of vane test observations is usually imperfect in the sense that some of the test results are reported not by their values but by the information that the values are larger than the measuring capacity of the applied vane. The corresponding random variables are said to be "clipped" at the capacity limits. This information is taken into account by integrating (23) with respect to each of the clipped variables in $\mathbf{x}_v$ from the corresponding capacity limit to ∞. Upon this integration and upon substituting the values observed to be below the corresponding capacity limits of the vanes, the right side of (23) defines the likelihood function of c, γ, and λ. The dependence of μ, σ, ρ, κ is not shown explicitely in (23).

Let (C,Γ,Λ) be the Bayesian random vector corresponding to (c,γ,λ) and adopt the non–informative prior for which $(C,\log\Gamma,\log(\Gamma^2+\sigma^2\Lambda^2))$ has a diffuse prior over $\mathbb{R} \times \{(\log\gamma,\log(\gamma^2+\sigma^2\lambda^2))\,|\,\gamma \in \mathbb{R}_+,\ 0\le\lambda\le1\}$. Then the prior density is proportional to $\lambda/[\gamma(\gamma^2+\sigma^2\lambda^2)]$, $(c,\gamma,\lambda) \in \mathbb{R} \times \mathbb{R}_+ \times [0,1]$ which multiplied on (23) (or its modification) gives the posterior density of (C,Γ,Λ). Fig. 7 shows contour curves in full line for the posterior joint density of (Γ,Λ) together with the two marginal density functions given that $C = 2.255$. This value of C is close to the point at which the posterior density of (C,Γ,Λ) is

maximal when μ,σ,ρ,κ are substituted by their maximum posterior density point estimates. The contour curves for the density as obtained by the product of the marginal distributions of Γ and Λ given C = 2.255 are shown by dotted lines, demonstrating the approximate independence of Γ and Λ. Further numerical studies of the joint posterior density of (C,Γ,Λ) and with variations of μ,σ,ρ,κ show that C in practice can be modeled to be independent of (Γ,Λ) and that C is Gaussian with E[C|M] = 1.827 + 0.453 M, D[C|M] = 0.081. For E[C|M = 0.946] = 2.255 this gives a mean of 9.57 and a coefficient of variation of about 8% for the ratio exp[C] = ("true" q_c)/("true" c_v).

This investigation is an illustrative example of how two quite inaccurate measuring methods applied to the same random object together give quantitative information about their individual measuring uncertainties and how this information can be used to separate the distributional properties of the random object from the measured properties.

The true in situ shear strength field Let $\eta(x,y,z)$ denote the "true" log c_v field (= log c_u field in situ). For given values of the parameters μ, σ, ρ, κ, c, and λ the field is Gaussian with (see (24) and (25) for $\gamma = 0$)

$$E[\eta(jh,y,z)\,|\,\zeta] = \lambda^2\{E[\zeta(jh,y,z)\,|\,\zeta]-\mu\} + \mu - c \tag{26}$$

$$\mathrm{Cov}[\eta(ih,y_1,z_1),\eta(jh,y_2,z_2)\,|\,\zeta] =$$

$$\lambda^2(1-\lambda^2)\,\mathrm{Cov}[\zeta(ih,y_1,z_1),\zeta(jh,y_2,z_2)] + \lambda^4\,\mathrm{Cov}[\zeta(ih,y_1,z_1),\zeta(jh,y_2,z_2)\,|\,\zeta] \tag{27}$$

The mean value function and the covariance function for the true undrained shear strength field are obtained from (26) and (27) by the standard transformation formulae between the parameters of the normal and the logarithmic normal distribution, Fig. 6 (right).

Fourth step: Strength increase due to consolidation Triaxial tests on clay till samples from Storebælt reveal that if the undrained shear strength $c_u(p_o)$ is known at some effective consolidation pressure level p_o, then it can be computed at another effective pressure level p by use of the formula

$$c_u(p)/c_u(p_o) = (p/p_o)^B \tag{28}$$

in which B can be modeled as a logarithmic normal random variable, Ditlevsen (1991d). The present data are not sufficient to determine the character of B as a random field over the soil body. Therefore two extreme cases are considered, the unconservative white noise case in which approximately only the mean E[B] contributes to the dissipation in the rupture figures, and the strongly conservative random variable case in which B is considered constant all over the soil body (in contradiction with the measurements, of course). In the last case the predictive distribution of B (that is, the distribution of B that includes the statistical uncertainty) should be used in the reliability evaluation. The formula (28) can be used with

p_0 being the known effective in situ consolidation pressure and $c_u(p_0)$ being the in situ shear strength field obtained as in the previous section while p is the effective consolidation pressure as it develops through the construction phase and ends up to in the finished state of the structure. This pressure p can be computed approximately on the basis of the elasticity theory.

Based on the assumption that B has a normal distribution, the present data allow the assignment $E[B] = 0.32 + 0.028\ T_{21.3}$, where $T_{21.3}$ is a random variable with t–density of 21.3 degrees of freedom. With the assumption that B has a logarithmic normal distribution this result will only be slightly conservative. The predictive Bayesian random variable log B can be assigned as $\log B = -1.21 + 0.39\ T_{10.7}$. Conditional on either $E[B] = \beta$ or $B = \beta$ the effect on the field of c_u as defined in the previous section is a multiplication by a non–random function.

Reliability computations After the fourth step the model for the quantitative random field descrition of the undrained soil shear strength is completed. The Bayesian random parameters to be used in (4) are $\theta_1 = M$, $\theta_2 = \Sigma$, $\theta_3 = K$, $\theta_4 = C$, $\theta_5 = \Lambda$, $\theta_6 = E[B]$ (or B). Upon a probabilistic modeling of the external work W a reliability analysis program e.g. as PROBAN (Veritas Sesam Systems) can be used to compute FORM or SORM approximations to the probability of the failure event (4) together with sensitivities with respect to all the relevant parameters. In each interation step the Monte Carlo integration technique is used as explained earlier to obtain the conditional mean and variance of the dissipation D. For each simulated sample point a kriging computation is needed. In principle this is a weighted summation over all measured values. However, only a part of these values (for Storebælt even a very minor part) contributes essentially to the sum. Therefore care should be taken in the computer program to economize at this point. Otherwise the computer time can be prohibitively long. Similarly it may be wise to apply importance sampling for the computation of the variance of the dissipation D.

Acknowledgements Professor Bent Hansen at the Department of Geology and Geotechnical Engineering, DTH has contributed with advice about rupture figures.

References

Brinch Hansen J. (1966). "Three–dimensional Effect in Stability Analysis", Bulletin No. 21, Danish Geotechnical Institute, Lyngby, Denmark.

Ditlevsen O. (1991a). "Stochastic Soil Strength Model for Reliability Analysis with Respect to Undrained Failure". (1991b). "Partitioning of Storebælt Clay Till Cone Tip Resistance Records in Population Components". (1991c). "Transformation of Cone Tip Resistance Measurements on Storebælt Clay Till into "True" in Situ Undrained Shear Strength". (1991d). "Consolidation Increment of Undrained Shear Strength of Storebælt Till Clay", Reports to AS Storebæltsforbindelsen, Copenhagen, Denmark.

Skempton, A.W. (1951). "The Bearing Capacity of Clays", Proc. Building Research Congress, London.